

Scanning tunnelling spectroscopy study of paramagnetic superconducting β' -
 $\text{ET}_4[(\text{H}_3\text{O})\text{Fe}(\text{C}_2\text{O}_4)_3]\cdot\text{C}_6\text{H}_5\text{Br}$ crystals

This article has been downloaded from IOPscience. Please scroll down to see the full text article.

2010 J. Phys.: Condens. Matter 22 175701

(<http://iopscience.iop.org/0953-8984/22/17/175701>)

View [the table of contents for this issue](#), or go to the [journal homepage](#) for more

Download details:

IP Address: 129.252.86.83

The article was downloaded on 30/05/2010 at 07:55

Please note that [terms and conditions apply](#).

Scanning tunnelling spectroscopy study of paramagnetic superconducting β'' -ET₄[(H₃O)Fe(C₂O₄)₃]·C₆H₅Br crystals

A Gambardella¹, M Salluzzo¹, R Di Capua^{1,2}, M Affronte³,
C Giménez-Saiz⁴, C J Gómez-García⁴, E Coronado⁴ and R Vaglio^{1,5}

¹ CNR-SPIN, Complesso Universitario di Monte S Angelo, Via Cinthia, 80126 Napoli, Italy

² Dipartimento S.p.e.S., Università degli Studi del Molise, Via De Sanctis, 86100 Campobasso, Italy

³ CNR-Institute of nanoSciences S3 and Dipartimento di Fisica, Università di Modena e Reggio Emilia, via G. Campi 213A, 41125 Modena, Italy

⁴ Instituto de Ciencia Molecular, Parque Científico, Universitat de Valencia, 46980 Paterna Valencia, Spain

⁵ Dipartimento di Scienze Fisiche, Università degli Studi di Napoli Federico II, Complesso Universitario di Monte S Angelo, Via Cinthia, 80126 Napoli, Italy

E-mail: roberto.dicapua@na.infn.it

Received 29 October 2009, in final form 11 March 2010

Published 7 April 2010

Online at stacks.iop.org/JPhysCM/22/175701

Abstract

Scanning tunnelling spectroscopy (STS) and microscopy (STM) were performed on the paramagnetic molecular superconductor β'' -ET₄[(H₃O)Fe(C₂O₄)₃]·C₆H₅Br. Under ambient pressure, this compound is located near the boundary separating superconducting and insulating phases of the phase diagram. In spite of a strongly reduced critical temperature T_c ($T_c = 4.0$ K at the onset, zero resistance at $T_c = 0.5$ K), the low temperature STS spectra taken in the superconducting regions show strong similarities with the higher T_c ET κ -derivatives series. We exploited different models for the density of states (DOS), with conventional and unconventional order parameters to take into account the role played by possible magnetic and non-magnetic disorder in the superconducting order parameter. The values of the superconducting order parameter obtained by the fitting procedure are close to the ones obtained on more metallic and higher T_c organic crystals and far above the BCS values, suggesting an intrinsic role of disorder in the superconductivity of organic superconductors and a further confirmation of the non-conventional superconductivity in such compounds.

(Some figures in this article are in colour only in the electronic version)

1. Introduction

Hybrid organic/inorganic superconductors having the formula BEDT-TTF_{*n*}X_{*m*}, where BEDT-TTF (or ET) is the organic donor bis(ethylenedithio)tetrathiafulvalene and X is an inorganic anion, are currently synthesized in a great variety of stable crystals in which alternating layers of ET and X are packed together. They differ one from another by their stoichiometry and packing patterns of the ET (the latter

denoted by an α , β , κ , ... placed before the compound name). κ -packed derivatives are the most studied so far due to their relatively high T_c values (10–15 K) among the ETs. All the members of this family attract a great deal of interest because of their peculiar physical properties. Some unusual aspects of the superconducting state, and in particular some unexpected similarities with the high critical temperature superconductors (HTS) [1], are really intriguing, among them the analogies between the phase diagrams (the

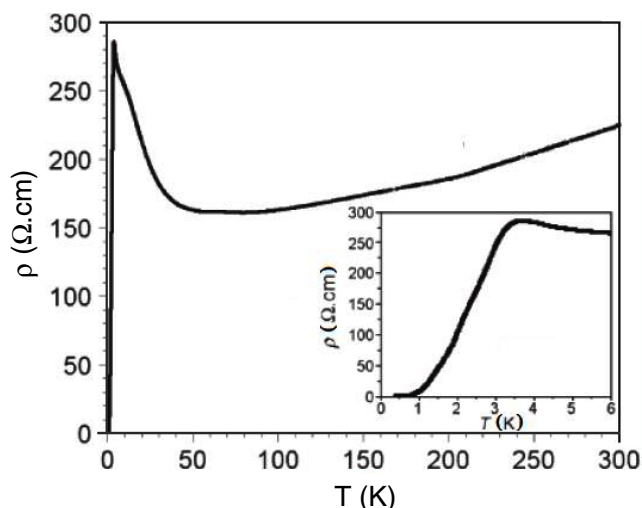


Figure 1. Typical resistivity versus temperature measurement for our β'' -ET₄[(H₃O)Fe(C₂O₄)₃]·C₆H₅Br crystals, showing the superconducting transition; the inset reports a magnification of the transition region.

pressure in the ETs having the role played by the doping in the HTSs), the huge anisotropy of the transport properties, and the indications for an unconventional order parameter [2]. Knight shift measurements [3, 4] and theoretical considerations on the particle–hole interaction (Bethe–Salpeter equation) [5] indicated that a singlet s- or d-wave state should describe the pairing symmetry. However, the experimental results [6–9] and their interpretation are still controversial. Nevertheless, the knowledge of the symmetry of the superconducting order parameter and more generally the superconductivity mechanisms in these compounds are still open questions.

An important characteristic of the ETs is the strong influence on the transport properties of the disorder associated with either the anion and/or the configuration of the ethylene groups within the donor layers. Indeed, the electronic properties are determined by the anion structure via short C–H–anion contact bonds of the terminal ethylene groups belonging to the ET molecules; in the synthesis of the solid, these terminal (CH₂)₂ groups can adopt two possible out-of-plane configurations, with the relative orientation of the outer C–C bonds being either eclipsed or staggered [10]. While at high temperatures the (CH₂)₂ system is thermally disordered, a preferential orientation in one of the two configurations, depending on the anion and crystal structure, is achieved when lowering the temperature. These molecular crystals often contain neutral guest molecules coming from the solvent, whose role must be considered in the low temperature state. Indeed, both the anion and the solvent molecule can affect the supramolecular organization of the ET molecules and influence the degree of ordering of their ethylene groups in the closer molecules, determining the stabilization of the superconducting state. Consequently, some intrinsic disorder might persist also at low temperature, suppressing the superconducting behaviour. Effects of disorder were extensively studied in κ -ET derivatives as a function of the cooling rate [11] or by deuteration [12], and a precise

evaluation of the residual disorder was recently done, also by considering the presence of additional degrees of freedom in determining glass-like transitions observed by changing the temperature [10]. Moreover, it has been suggested that the presence of magnetic ions could play some role in the superconducting state, especially in the suppression of the critical temperature (T_c), and some studies emphasized the role played by intrinsic disorder in the members of the β'' -ET₄[(H₃O)M(C₂O₄)₃]·C₆H₅N family with M = Ga, Cr, Fe [13–15].

Scanning tunnelling spectroscopy (STS) represents a powerful technique providing information, on a local scale, about the role of intrinsic disorder and/or the presence of magnetic layers on the ET derivatives superconducting properties. Here we report a low temperature STS investigation on a new member of the β'' -ET₄[(H₃O)M(C₂O₄)₃]·G family, where M is a metal transition atom and G is the guest molecule [16]. Early STS studies on ETs were mainly addressed to determine their superconducting order parameter by fitting the experimental curves with s- or d-wave models for the density of states (DOS) [17, 18], and in the latter case also by checking the angular dependence of the supposed gap anisotropy [19]. Nevertheless, STS studies did not evidence a possible role, in the low temperature properties, of the intrinsic disorder in the ethylene group, of the effect of paramagnetic ions in the neighbour anionic layer, and in general of the characteristics of the order parameter symmetry.

In this paper we focus on the STS study of β'' -ET₄[(H₃O)Fe(C₂O₄)₃]·C₆H₅Br. Under ambient pressure, this compound is located at the boundary between the superconducting and insulating phases of the phase diagram. We observed STS spectra similar to those previously measured on κ -derivatives characterized by higher T_c . This finding suggests that there is not a strong suppression of the amplitude of the order parameter in the ETs approaching the superconducting–insulating transition in the phase diagram. Moreover, considering the critical temperature, the values of estimated superconducting gap are far above the BCS prediction. We compared our spectroscopic curves with different microscopic models: the Abrikosov–Gorkov model valid for a superconductor in the presence of paramagnetic impurities in an s-wave scenario, a d-wave model with non-magnetic impurities, and a modified d-wave model affected by disorder as suggested by the behaviour of the high T_c superconductors. The results suggest an intrinsic role of the disorder in the superconductivity of ETs derivative superconducting compounds.

2. Experimental details

2.1. Samples

Single crystals of β'' -ET₄[(H₃O)Fe(C₂O₄)₃]·C₆H₅Br were synthesized according to a procedure described elsewhere [16]; they are typically prismatic rods, about $2 \times 1 \times 0.1$ mm³ in size. The crystal orientation was determined by x-ray diffraction.

The transport properties of the single crystals show metallic behaviour down to 100 K, an intermediate insulating

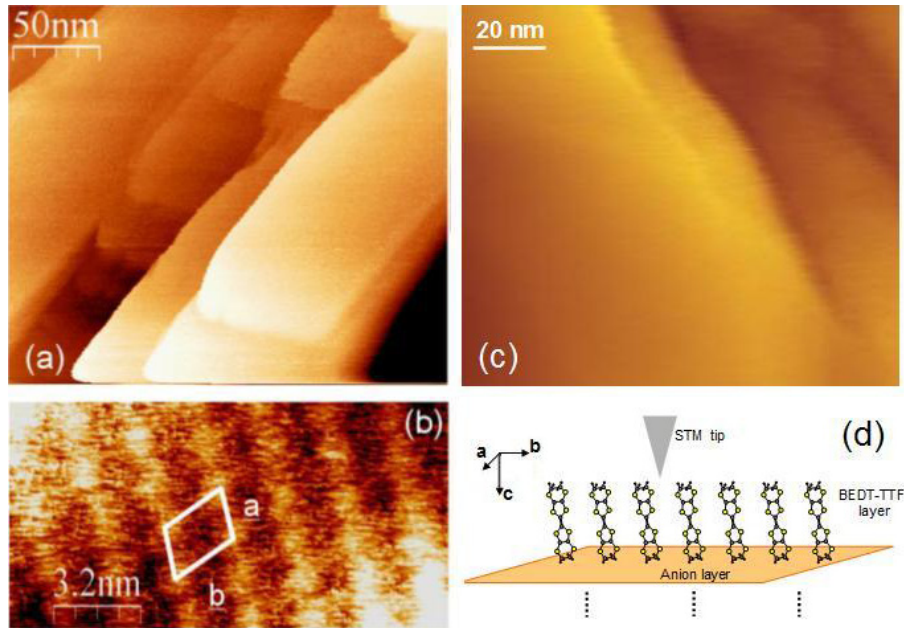


Figure 2. (a) STM topography showing molecularly flat terraces obtained at room temperature (298 K) using the UHV VT-AFM Omicron system, acquired at $I_T = 2$ pA and $V_{\text{bias}} = 1.5$ V in ultra-high vacuum conditions. (b) Molecular resolution image obtained in the same conditions showing the ab unit cell of the crystal. (c) STM topography showing molecularly flat terraces obtained at 4.2 K using the home-made cryogenic system, acquired at $I_T = 50$ pA and $V_{\text{bias}} = 1.0$ V in pure He gas. (d) Sketch of the experimental configuration, showing the tip position with respect to the crystal orientation; the scan direction is parallel to the ab plane.

regime, and a superconducting transition with an onset T_c at 4.0 K and a full transition at 0.5 K, as determined by resistivity versus temperature measurements (figure 1).

STM–STS measurements were performed on the crystal surface oriented along the ab plane, which is parallel to the ET molecular plane.

2.2. Room temperature STM

Topographic measurements at room temperature were performed in ultra-high vacuum (UHV) with a commercial Omicron VT-AFM scanning tunnelling microscope, using tungsten commercial tips. After a short ultrasonic exposure to pure demineralized water, molecular resolution was obtained, with a tip to sample voltage of 1 or 2 V at a tunnel current of 1 or 2 pA. Typical tunnel resistances were therefore of the order of 1 T Ω .

Topographic images with molecular resolution were recorded after some low temperature measurement runs, without applying any particular surface treatment or cleaving. These findings proved that surfaces of our single crystals are relatively stable.

2.3. Low temperature STS

For the STS measurements we used a home-made STM able to operate in a cryogenic environment. The lowest achieved experimental temperature (measured on the sample stage) was 1.3 K, reached by pumping on the liquid helium in the sample chamber. Temperatures between 1.3 and 4 K were stabilized by tuning the pumping through a mechanical valve. The temperature stability, together with the short time required to

acquire some spectra in a surface location (tenth of seconds), allows to measure good quality, low noise, tunnel spectra. Clean samples were mounted on the scanner in a glove box under continuous flux of inert pure helium gas, and then sealed in helium atmosphere to preserve surface quality and avoid condensation at low temperature. Platinum–iridium tips, electrochemically etched, were used.

The reproducibility of the normalized spectra at different tunnel resistances ensures the high quality of the junction. The differential tunnelling conductance dI/dV was measured by a standard lock-in technique. Typical tunnelling spectra on different samples obtained from different batches were recorded by stabilizing the STM junction at bias voltages between 30 and 100 mV and tunnelling currents below 300 pA. Thus, in such measurements the STS junction was stabilized at tunnel resistances of about 100 M Ω , about four orders of magnitude lower than in room temperature topographic images with molecular resolution.

The extremely different tunnel resistance ranges of the optimal working of the two instruments prevented us from realizing molecular resolved topographies at low temperatures, since our cryogenic system and electronics are not designed to work at the high tunnel resistance and low tunnel current used on the Omicron VT-AFM.

3. Results and discussion

Room temperature STM–UHV images of the crystal surface, obtained by the Omicron VT-AFM system, are shown in figures 2(a) and (b), while figure 2(c) shows a topographic image at 4.2 K recorded by the home-made cryogenic STM.

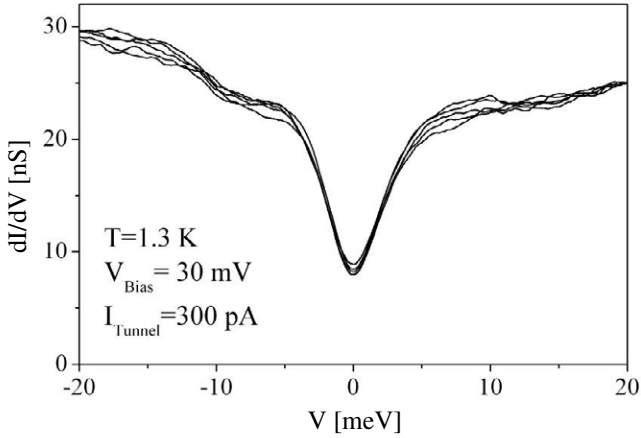


Figure 3. Raw data STS spectra recorded at $T = 1.3$ K showing the high reproducibility of the superconducting spectra. The curves were taken within the same superconducting region in different surface locations.

Figure 2(d) shows a scheme of the experimental set-up that shows the position of the tip with respect to the crystalline planes as previously determined by x-ray measurements. The typical surface morphologies exhibit flat ab terraces, separated by one or multiple unit cell steps (the measured height for each step is about 3 nm, corresponding to the c -axis). Figure 2(b) shows a molecular resolution image, not yet reported on this β'' -derivative in the literature; a slight surface distortion of the unit cell was found as in earlier STM observations on an ET derivative having a β -packing motif [20].

Low temperature (1.4 K) spectroscopy measurements show that, sweeping the tip on different positions of these ab terraces, regions with different superconducting dI/dV spectra, or even semiconducting regions, can be identified. This suggests that at microscopic scale the sample is not fully homogeneous; such inhomogeneity in the isostructural β'' -phases is already known [15], and could easily explain the large width of the superconducting transition (from 4 to 0.5 K) of our samples. However, we focused our attention only on large superconducting ab terraces where spectra like those shown in figures 3 and 4 were reproducibly observed. Similar results are found on other batches of samples.

We found a non-linear background in the dI/dV characteristics, with an approximated parabolic shape, similar to what is observed on superconducting ETs like κ - $\text{ET}_2\text{Cu}(\text{NCS})_2$ having T_c up to 12 K [17–19]. This parabolic background can arise from a contribution to the tunnelling coming from non-superconducting layers. Due to the anisotropic structure, the crystal surface could terminate with either the inorganic layer or the ET superconducting molecular groups. Another important common characteristic of the STS spectra measured on our crystals and other STS data on ETs organic superconductors is the presence of much broadened coherence peaks and a high zero bias conductance. Although it is likely that several factors may contribute to this ubiquitous broadening, including extrinsic features of the surface [21], here we focus on the intrinsic residual disorder characteristic of the ET compounds. Recent transport

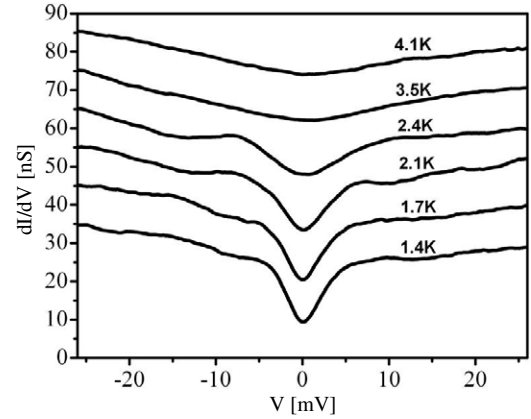


Figure 4. dI/dV versus V spectra (raw data, averaged at the same location) taken within the same region and at variable temperature showing the broadening of the spectra and the disappearance of the gap close to the value of the onset T_c of about 4 K. Curves are shifted by 10 nS for clarity.

measurements on β'' - ET_4 family compounds also pointed out the intrinsically inhomogeneous nature of these systems, suggesting the presence of a mixed metallic insulating state at low temperatures due to residual disorder (or impurities) [15].

Indeed, at low temperatures the observed tunnelling spectra could be related to the residual disorder of the ethylene groups in the ET molecules and to the disorder of the anions.

Spectra taken at different locations within the same region of the crystal are shown in figure 3. They show features that can be summarized as follows: an asymmetric background, with higher conductivity for negative bias voltages on the sample; broad peaks at about 6 meV; strong conductivity depression below 6 meV. The temperature dependence of the STS spectra from the same region (on the largest terrace in figure 2(c)) is reported in figure 4. The spectra continuously broaden at temperatures above 2.5 K. Since we do not have molecular resolution at low temperature, we cannot exclude that a displacement at molecular level (caused by thermal drift) contributed to the slight differences in the ‘peak’ behaviour at lower temperature. However, the spectra recorded in different superconducting regions at fixed temperature, reported in figure 3, prove that the differences among them are beyond the details at which our quantitative analysis is developed, as shown in the following. A small suppression of the density of states is still present at 4.1 K, but any sign of a coherence peak disappears already above 3.5 K. The temperature dependence of the spectra is consistent with the onset T_c of the compound [16]. This result suggests that these regions are superconducting, and the spectra are characteristic of the superconducting properties of the sample.

In order to compare the experimental data with various microscopic models for the superconductivity, we have used the general expression of the tunnelling conductance, $G_S(V) = dI/dV$, as a function of the superconducting density of states (DOS) $N(E)$ [22]:

$$\frac{G_S(V)}{G_N} = \int_{-\infty}^{\infty} \frac{N_S(E)}{N_N(0)} \frac{df(E - eV)}{d(eV)} dE. \quad (1)$$

Here E is the energy ($E = 0$ being the Fermi level), G_N is the normal state conductance of the tunnel junction, $N_N(0)$ is the density of states in the normal state at the Fermi level and $f(E)$ is the Fermi distribution function.

The strong peak smearing, together with the relatively large energy interval and low dI/dV values of the conductivity depression around the Fermi level at 1.4 K, makes impossible a reliable fit of the spectra by using a conventional s-wave DOS with Dynes broadening parameter.

A way to model the disorder in the conductance spectra, and therefore to reproduce the peak smearing and the zero bias conductance, is to consider the presence of scattering centres, which hinder superconductivity and create pair breaking. The role played by disorder can be taken into account within a conventional framework for superconductivity by using the Abrikosov–Gorkov (AG) model that describes the suppression of T_c due to magnetic impurities. The AG model also describes the effect of non-magnetic scattering centres in d-wave superconductors (in the weak limit). In the frame of the AG theory [23], the effect of magnetic impurities on the energy spectrum can be evaluated, and an appropriate expression for the DOS can be inferred. The main prediction is the rising of a gapless superconductivity when the paramagnetic concentration is high enough. An approximate expression for the DOS in this case is given by [24]

$$N_S(E) \propto 1 + \frac{1}{2} \frac{(E/\Delta_G)^2 - \alpha^2}{[(E/\Delta_G)^2 + \alpha^2]^2} \quad (2)$$

where Δ_G is the (temperature-dependent) AG order parameter, which no longer represents an energy gap in the quasi-particle excitation spectrum; α is proportional to n_i/Δ_G , n_i being the concentration of paramagnetic impurities.

In the case of non-magnetic impurities as pair-breakers in an unconventional framework, the simplest approach is to consider the d-wave model formula for the DOS:

$$N_S(E) \propto \frac{1}{2\pi} \int_0^{2\pi} \left| \text{Re} \frac{E - i\Gamma}{\sqrt{(E - i\Gamma)^2 - \Delta(\theta)^2}} d\theta \right| \quad (3)$$

where Γ is the Dynes broadening parameter, θ the azimuthal angle in the reciprocal space, and $\Delta(\theta)$ the gap as a function of the \mathbf{k} -vector. In the simple $d_{x^2-y^2}$ -wave model, $\Delta(\theta) = \Delta_0 \cos 2\theta$.

In order to get a better description of tunnelling data on HTS samples, Alldredge *et al* used a modification of the d-wave model to reproduce the DOS of superconducting $\text{Bi}_2\text{Sr}_2\text{CaCu}_2\text{O}_{8+\delta}$ crystals characterized by various dopings [25]. They showed that the tunnel spectra, throughout most of the $\text{Bi}_2\text{Sr}_2\text{CaCu}_2\text{O}_{8+\delta}$ phase diagram, are well fitted if, besides an anisotropic energy gap $\Delta(\mathbf{k})$, an energy-dependent scattering rate $\Gamma(E) = a \cdot E$ is introduced.

We also used such a ‘modified d-wave’ model as a third possibility for the DOS, using a linearly energy-dependent scattering term, $\Gamma = \Gamma(E)$, having the form $\Gamma(E) = \Gamma_r + |a \cdot E|$. Within this phenomenological approach, Γ_r corresponds to the presence of a persistent contribution to the particle density of states probably due to residual disorder.

In figure 5 a comparison between the above-mentioned three models is shown (the least square fit was performed for

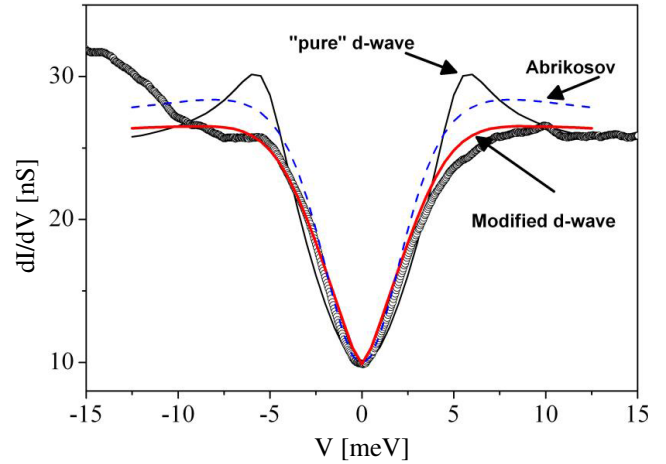


Figure 5. Comparison between the experimental data (open circles, $T = 1.3$ K, curve normalized to the curve acquired in the same location at 4.1 K), and theoretical models: pure d-wave (black continuous line), Abrikosov–Gorkov (blue dashed line) and the modified d-wave model (red continuous line). Note the different agreement in the region of the coherence peaks between the experimental data and the models taking disorder into account.

$|V| < 10$ mV, to prevent the results being affected by the rise of the spectrum below -10 mV).

As observed in previous works [17–19], the ‘pure’ d-wave fitting result is reliable only in the energy region close to the Fermi energy, while it fails in describing the lack of coherence peaks. Equation (3) is not able to reproduce the effect of impurities or disorder on the suppression of the superconductivity (whose effects are generically included in the Dynes broadening parameter). This is not surprising, since even in HTS single crystals it is relatively difficult to find a good agreement with the experimental DOS and the prediction of the clean d-wave model.

If compared with the pure d-wave model, a better agreement between the experimental data and the theory is obtained through the AG model and the modified d-wave model; the latter better reproduces the pronounced smearing of the coherence peaks (but it also has one fitting parameter more), where the AG model exhibits its larger discrepancies. The values of the energy gap found in the models are $\Delta = 5.3 \pm 0.2$ and $\Delta = 5.9 \pm 0.2$ meV for the d-wave and modified d-wave models respectively, and 6 meV in the case of the AG model (although it should be recalled that in the AG model the value of Δ does not represent an energy gap).

Several assertions can be inferred from our analysis.

First, it is clear from our fittings that models taking into account the effects of disorder better reproduce the experimental data. The coherence peak smearing in the dI/dV characteristics seems to be recognizable as an intrinsic feature of BEDT-TTF superconductors; nevertheless, this smearing has to be taken into account in both an s-wave or d-wave scenario besides its magnetic or non-magnetic nature. The effects of disorder seem to be intrinsic in these organic superconductors, being directly linked to the presence of the ET group and/or to their interaction with the anionic layer.

Second, the values of the order parameter obtained from the models produce a high $2\Delta/kT_c$ ratio (30–35, with

$T_c = 4$ K) far from the BCS values even for a clean d-wave order parameter.

Such a high ratio is not frequently observed even in the HTSs, where values around ten are common and higher values are observed corresponding to opening of a gap in the DOS around the Fermi level above the critical temperature, known as a pseudogap. This could suggest a pseudogap effect rather than a superconducting gap in our samples also. However, it must be pointed out that the opening of a gap at about 6 meV in the dI/dV curves reported here disappears above the onset T_c . It resembles what was observed by Kugler *et al* [26] on overdoped $\text{Bi}_2\text{Sr}_2\text{CuO}_{6+\delta}$ (Bi2201): they measured a $2\Delta/kT_c$ ratio of about 28, arguing from the temperature behaviour that it was related to a superconducting gap and not to a pseudogap. The same group measured on the same compound an even higher ratio (data not published, but cited in [27]). Bi2201 is a compound of the same family of $\text{Bi}_2\text{Sr}_2\text{CaCu}_2\text{O}_{6+\delta}$ (Bi2212), but with a lower T_c and much less studied; the ratio between T_c values being higher than the ratio of the gaps, a high $2\Delta/kT_c$ value occurs. This is a further similarity with our case, if we compare the features of our compound with those of the higher T_c compounds of the same class. Other very high $2\Delta/kT_c$ ratios have been observed: almost 60 on Pb-doped Bi2201 [28], around 20 or higher on Bi2212 [25, 29, 30]. In these cases, however, the attribution to a superconducting gap or to a pseudogap was considered controversial by the authors themselves; basically, such values were related to nanoscale inhomogeneities and granularities on the sample surfaces, and the authors discussed a phase separation between superconducting (exhibiting lower ratios) and pseudogap regions, without claiming a strong conclusion since they did not follow the temperature behaviour up to T_c . In our case, on the contrary, we observed a separation between regions with semiconducting character and other regions having superconducting behaviour; in the latter, we observed the disappearance close to T_c of the structures measured at lower temperatures. Following such argumentations, we attribute the spectral inhomogeneous behaviour (superconducting or semiconducting) to the intrinsic disorder of the compounds of this family and/or to superconducting fluctuations rather than a surface granularity; the high $2\Delta/kT_c$ ratio seems to be a consequence of a non-conventional superconducting gap rather than be ascribable to a pseudogap feature.

The presence of the superconducting (S) and the Mott insulating (MI) phases are common features in the phase diagrams of organic superconductors (as well as for HTSs). A phase diagram for the compound we studied is not yet available. However, the reduced T_c despite the still large gap value suggests that $\beta''\text{-ET}_4[(\text{H}_3\text{O})\text{Fe}(\text{C}_2\text{O}_4)_3]\cdot\text{C}_6\text{H}_5\text{Br}$, like other compounds of the BEDT family, is at ambient pressure in the proximity of the S–MI transition; i.e., it has a low t/U value (t being the tight binding transfer integral and U the on-site Coulomb repulsion) close to the boundary separating superconducting and Mott insulating phases, but still large enough to prevent the Coulomb correlations to dominate the ground state properties. The temperature dependence of the resistivity is consistent with this hypothesis: a metallic-like behaviour at high temperature (T^2), an insulating

behaviour below 50 K, and a peak before the superconducting transition, all characteristics common in HTSs close to the superconducting–insulating transition. In HTSs the role of phase fluctuations have been recognized to play an important role in explaining the S–I transition. We notice that, in our $\beta''\text{-ET}_4[(\text{H}_3\text{O})\text{Fe}(\text{C}_2\text{O}_4)_3]\cdot\text{C}_6\text{H}_5\text{Br}$, which is located at the boundary of the S–I transition, the value for the gap is similar to those obtained on derivatives with higher T_c , which do not show the anomalous temperature dependence of the resistivity observed in our case, and that are located in the superconducting dome but far from the boundary of the phase diagram. This result suggests that the amplitude of the order parameter is not suppressed going from the superconducting to the insulating phase, as happens in the HTSs. This is opposite to the conventional BCS scenario, where the effect of disorder on a two-dimensional system should result in a suppression of the amplitude of the order parameter, as observed in amorphous Bi films [31]. All this findings are consistent with the idea that also in this family of superconductors the S–I transition is due to phase fluctuations of the order parameter; the key role played by such fluctuations when approaching the insulating to superconducting transition (as in cuprates) has been clearly discussed in [32].

4. Conclusions

When STS is performed on $\beta''\text{-ET}_4[(\text{H}_3\text{O})\text{Fe}(\text{C}_2\text{O}_4)_3]\cdot\text{C}_6\text{H}_5\text{Br}$ crystals, the characteristics of the measured spectra are found to be similar to what is observed on ET compounds with higher T_c values.

The broadened characteristics suggest that the presence of residual disorder at low temperature could give rise to the coexistence of superconducting and insulating phases, and could play some role in influencing the superconducting state. Indeed, when models involving the presence of magnetic and non-magnetic impurities are invoked, they are found to be in better agreement with the experimental DOS.

The residual disorder can probably be ascribed to the ordering of terminal ethylene groups in the ET molecule and/or the anion, even if we cannot exclude a phase separation triggered by a charge density wave transition or an influence from the solvent molecules (often embedded in such compounds). Together with the AG model for describing the suppression of superconductivity due to magnetic impurities in a conventional scenario, we considered a modified d-wave model, in which a linearly energy-dependent broadening parameter was used to fit the experimental DOS, finding a general better agreement with the data. In particular, we observed a lack of suppression of the order parameter in $\beta''\text{-ET}_4[(\text{H}_3\text{O})\text{Fe}(\text{C}_2\text{O}_4)_3]\cdot\text{C}_6\text{H}_5\text{Br}$ crystals compared to the higher T_c ET compounds, pointing to unconventional superconducting behaviour.

Acknowledgments

This work was carried out within the framework of the Network of Excellence MAGMANet supported by the EC under contract No 515767. The work in Spain was supported

by the Spanish Ministry of Science and Innovation (Project Consolider-Ingenio in Molecular Nanoscience, CSD2007-00010, and MAT2007-61584).

References

- [1] Kagawa F, Miyagawa K and Kanoda K 2005 *Nature* **436** 534–7
- [2] Wosnitza J 2007 *J. Low Temp. Phys.* **146** 641–67
- [3] De Soto S M, Slichter C P, Kini A M, Wang H H, Geiser U and Williams J M 1995 *Phys. Rev. B* **52** 10364–8
- [4] Mayaffre H, Wzietek P, Jerome D, Lenoir C and Batail P 1995 *Phys. Rev. Lett.* **75** 4122–5
- [5] Vojta M and Dagotto E 1999 *Phys. Rev. B* **59** R713–6
- [6] Carrington A, Bonalde I J, Prozorov R, Giannetta R W, Kini A M, Schlueter J, Wang H H, Geiser U and Williams J M 1999 *Phys. Rev. Lett.* **83** 4172–5
- [7] Pinteric M, Tomic S, Prester M, Drobac D J, Milat O, Maki K, Schweitzer D, Heinen I and Strunz W 2000 *Phys. Rev. B* **61** 7033–8
- [8] Elsinger H, Wosnitza J, Wanka S, Hagel J, Schweitzer D and Strunz W 2000 *Phys. Rev. Lett.* **84** 6098–101
- [9] Gambardella A, Di Capua R, Salluzzo M, Vaglio R, Affronte M, del Pennino U, Curreli S, Giménez-Saiz C, Gómez-García C J and Coronado E 2008 *Solid State Sci.* **10** 1773–6
- [10] Wolter A U B, Feyerherm R, Dudzik E, Sullow S, Strack C, Lang M and Schweitzer D 2007 *Phys. Rev. B* **75** 104512
- [11] Pinteric M, Tomi S, Prester M, Drobac D and Maki K 2002 *Phys. Rev. B* **66** 174521
- [12] Oizumi H, Sasaki T, Yoneyama N and Kobayashi N 2006 *J. Phys.: Conf. Ser.* **51** 323–6
- [13] Powell B J and McKenzie R H 2004 *Phys. Rev. B* **69** 024519
- [14] Bangura A F, Coldea A I, Singleton J, Ardavan A, Akutsu-Sato A, Akutsu H, Turner S S, Day P, Yamamoto T and Yakushi K 2005 *Phys. Rev. B* **72** 014543
- [15] Coldea A I, Bangura A F, Singleton J, Ardavan A, Akutsu-Sato A, Akutsu H, Turner S S and Day P 2004 *Phys. Rev. B* **69** 085112
- [16] Coronado E, Curreli S, Giménez-Saiz C and Gómez-García C J 2005 *J. Mater. Chem.* **15** 1429–36
- [17] Arai T, Ichimura K, Nomura K, Takasaki S, Yamada J, Nakatsuji S and Anzai H 2001 *Phys. Rev. B* **63** 104518
- [18] Ichimura K, Higashi S, Nomura K and Kawamoto A 2005 *Synth. Met.* **153** 409–12
- [19] Arai T, Ichimura K, Nomura K, Takasaki S, Yamada J, Nakatsuji S and Anzai H 2001 *Synth. Met.* **120** 707–8
- [20] Renner C and Fischer Ø 1995 *Phys. Rev. B* **51** 9208–18
- [21] Gorczyca A, Krawiec M, Maska M M and Mierzejewski M 2007 *Phys. Status Solidi b* **244** 2448–52
- [22] Tinkham M 1996 *Introduction to Superconductivity* 2nd edn (New York: McGraw-Hill) p 76
- [23] Abrikosov A A and Gor'kov L P 1961 *Sov. Phys.—JETP* **12** 1243
- [24] Ambegaokar V and Griffin A 1965 *Phys. Rev.* **137** A1151–67
- [25] Alldredge J W, Lee J, McElroy K, Wang M, Fujita K, Kohsaka Y, Taylor C, Eisaki H, Uchida S, Hirschfeld P J and Davis J C 2008 *Nat. Phys.* **4** 319–26
- [26] Kugler M, Fisher Ø, Renner C, Ono S and Ando Y 2001 *Phys. Rev. Lett.* **86** 4911
- [27] Fisher Ø, Kugler M, Maggio-Aprile I and Berthod C 2007 *Rev. Mod. Phys.* **79** 353
- [28] Mashima H, Kinoda G, Ikuta H and Hasegawa T 2003 *Physica C* **388/389** 275
- [29] Matsuda A, Fujii T and Watanabe T 2003 *Physica C* **388/389** 275
- [30] McElroy K, Lee D H, Hoffmann J E, Lang K M, Lee J, Hudson E W, Eisaki H, Uchida S and Davis J C 2005 *Phys. Rev. Lett.* **94** 197005
- [31] Valles J M Jr, Dynes R C and Garno J P 1992 *Phys. Rev. Lett.* **69** 3567–70
- [32] Nam M-S, Blundell S J, Schlueter J A and Ardavan A 2007 *Nature* **449** 584–7